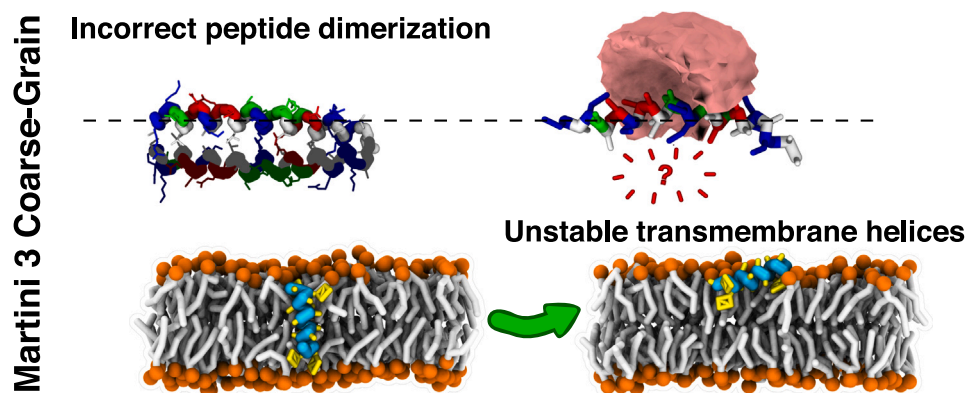Research paper

Room for improvement in the initial martini 3 parameterization of peptide interactions

J. Karl Spinti, Fernando Neiva Nunes, Manuel N. Melo *

Instituto de Tecnologia Química e Biológica António Xavier, Universidade Nova de Lisboa, Av. da República, 2780-157, Oeiras, Portugal

GRAPHICAL ABSTRACT

HIGHLIGHTS

- Martini 3 coarse-grain fails to capture coiled-coil helix dimerization.
- Helix contacts are sparse and occur via wrong interfaces.
- Martini 3 recovers transmembrane helix tilt dependency on thickness mismatch.
- A possible hydrophobicity imbalance drives out helices from the membrane core.

ARTICLE INFO

ABSTRACT

The Martini 3 coarse-grain force field has greatly improved upon its predecessor, having already been successfully employed in several applications. Here, we gauge the accuracy of Martini 2 and 3 protein interactions in two types of systems: coiled coil peptide dimers in water and transmembrane peptides. Coiled coil dimers form incorrectly under Martini 2 and not at all under Martini 3. With transmembrane peptides, Martini 3 represents better the membrane thickness–peptide tilt relationship, but shorter peptides do not remain transmembranar. We discuss related observations, and describe mitigation strategies involving either scaling interactions or restraining the system.

---

* Corresponding author.
  E-mail address: m.n.melo@itqb.unl.pt (M.N. Melo).
  URL: https://www.itqb.unl.pt/labs/multiscale-modeling/ (M.N. Melo).

1. Introduction

The past decade has seen an explosion in the adoption of coarse-grain (CG) molecular dynamics (MD) [1]. By employing reduced-dimensionality models one can lower the computational costs of MD simulations by several orders of magnitude, and bring into reach timescales of milliseconds and size scales approaching the micrometer [1]. The Martini force field has been at the forefront of many important CG MD applications [1] and is arguably the most used such model for biomolecular simulations. This is not to say CG models like Martini — where simplification is achieved by representing groups of about 4 non-hydrogen atoms as single particles, or "beads" — are without limitations: besides obvious trade-offs, such as the inability to represent fine chirality or explicit hydrogen-bonding, Martini often suffered from 'overmapping', a condition in which models with mappings finer than 4-to-1 led to imbalanced hydrophobic/hydrophilic interactions [2].

The recently-released Martini 3 model [3] tackles the limitations of the prior Martini 2 model [4–6] by introducing several new particle types, with explicitly different interaction sizes to account for 3-to-1 and 2-to-1 mappings. With this new approach proteins in solution, transmembrane (TM) pores, and helical membrane-bound oligomers have been successfully simulated without undergoing excessive protein aggregation [3] as was likely under Martini 2 [2,7–9]. With over-aggregation out of the way, we set out in this work to gauge the accuracy of more subtle aspects of Martini 3 protein interactions. We focus on two types of biologically relevant systems: (i) coiled-coil dimers with well-defined parallel structures [10,11] (PDB ids 1ZIK and 1U0I) to test Martini 3 recognition of heptad repeats — an aspect strongly dependent on steric matching and hydrophobicity/hydrophilicity discrimination [12]; and (ii) the WALP (tryptophan–alanine–leucine) series of peptides, which are single-pass TM alpha-helices with a well described tilting behavior in response to membrane thinning [13–15]. The study of the latter systems was prompted by recent observations that transmembranar behavior might be somewhat unstable under Martini 3 [16,17].

In this work we compare the Martini 2 and 3 behavior of the examined systems to experimental data and observations with finer models to identify aspects in which Martini 3 can be improved. This is relevant as Martini 3 proteins and lipids have not yet been parameterized to fully take advantage of the possibilities of the new model, and our findings can then be considered in upcoming developments.

2. Methods

2.1. Topology generation

All the peptides used in this work are alpha-helical. Their Martini 2.2 and Martini 3 CG topologies were created from atomistic structures (see Table 1 for sequences) using the martinize2 [18] script. For the coiled coil systems, the GCN4-leucine zipper mutant N16K parallel homodimer [11] (PDB id: 1ZIK) and the IAAL-E3/K3 synthetic parallel heterodimer [10] (PDB id: 1U0I, model 1/20) were used as starting points; Martini 2 and 3 topologies were generated using angle/torsion restraints to enforce helicity. These were our base systems to study dimerization behavior. For Martini 3, additional topologies were created: (i) with added elastic restraint networks using martinize2's default parameters, and (ii) with 40% stronger (700 kJ/mol/nm^2) elastic restraint networks together with side-chain orientation restraints [19]. For the TM WALPs, ideal α-helical structures were created from their sequence using the Avogadro software [20] and the Martini 2/3 topologies constructed using only angle/torsion secondary structure restraints. WALPs are capped on both termini, with N-terminal acetylation and C-terminal *n*-methyl amidation [13] (Table 1); since neither capping group has been explicitly parameterized for Martini, we modeled them by simply assigning a non-charged, random-coil, backbone particle type to the WALP's terminal beads (type P5 in Martini 2 and P2 in Martini 3).

Table 1
Amino acid sequences of the simulated peptides.

Peptide	Sequence
WALP16[a]	GWW(LA)$_5$WWA
WALP19[a]	GWW(LA)$_6$LWWA
WALP23[a]	GWW(LA)$_8$LWWA
WALP27[a]	GWW(LA)$_{10}$LWWA
1ZIK	RMKQLEDKVEELLSKKYHLENEVARLKKLV
1U0I-A	EIAALEKEIAALEKEIAALEK
1U0I-B	KIAALKEKIAALKEKIAALKE

[a]WALP peptides are termini-capped with N-terminal acetylations and C-terminal *n*-methyl amidations [13].

2.2. System setup

For the coiled coil peptides the two monomers comprising each dimer were separated by 4 nm and oriented randomly. Dimers were then solvated in a dodecahedral box of vector length 11.4 nm, with 0.15 M added NaCl, plus neutralizing Cl$^-$ counterions for the 1ZIK system. Additional systems were simulated in the same conditions, except peptides started in their dimeric configuration, directly coarse-grained from the respective PDB structure.

The WALP peptides were aligned vertically (with N terminus pointing upward) in order to start the simulation in ideal TM configurations. The peptides were then overlapped with a 10×10 nm^2 square membrane of DMPC phospholipids (dimirystoylphosphatidylcholine), with 9 nm simulation box height, built using the `insane.py` script [21]. Water was added to fill the box, together with an NaCl ionic strength of 0.15 M. In the Martini 2 systems, 10% of water beads were changed to the 'antifreeze' type to prevent freezing, as recommended [4].

For umbrella-sampling of the TM-to-adsorbed transition of WALP16, 45 windows were simulated, with Martini 2 and 3, at different depths of the peptide's N terminus (from 2.1 to −2.3 nm z-distance relative to the bilayer center). To generate starting structures for each window a simulation was carried out progressively restraining the N terminus to depths closer to the C terminus, with periodic output of structures. Starting configurations were selected from these structures, as the closest to each window's target depth.

2.3. Simulation conditions

Unbiased simulations were carried out in triplicate, for a minimum 23 μs per replicate, for a total simulation time beyond 3 ms (some replicates were simulated significantly longer than others; see Supplementary Table S1). The GROMACS 2020 simulation package [22] was used with a Verlet neighborlist scheme, at a 20 fs time-step. Typical Martini settings were used for nonbonded interactions [23]: Lennard-Jones and Coulombic potentials were cut-off at 1.1 nm, with Coulombic interactions further treated under a reaction-field scheme with a dielectric constant of 15. Temperature was kept at 300 K by a V-rescale thermostat [24] with a 1 ps coupling time. A Parrinello–Rahman barostat [25] with 12 ps coupling time was used to maintain pressure at 1 bar; pressure was coupled isotropically and semi-isotropically (independently in the xy and z directions) for the coiled-coil systems and WALP/membrane systems, respectively. After system assembly and energy-minimization, but prior to production runs, a 2 ns pressure/temperature equilibration was run for all systems, using the more robust Berendsen barostat [26] with a relaxation time of 3 ps.

Umbrella-sampling simulations of WALP16 followed the same setup as for unbiased simulations, for 1 μs per window. A quadratic potential of force 500 kJ/mol/nm^2 was added on the N-terminal backbone bead, restraining it to each window's target depth relative to the center-of-mass of the membrane. To prevent translocation of the C terminus during sampling, a repulsive half-harmonic potential with onset at the center of the membrane was added, affecting only the C-terminal backbone bead.

2.4. System manipulation, analysis and visualization

Peptide alignment and trajectory analysis was done primarily using the MDAnalysis [27,28] and NumPy [29] Python packages, together with matplotlib [30] for plotting and VMD version 1.9.3 [31] for molecular visualization and rendering. Tilt angles were computed using the HELANAL algorithm [32] as implemented in MDAnalysis. Because the simulated membranes may undergo a small degree of buckling, thicknesses were computed patch-wise, using the binning implemented in the LiPyphilic Python package [33]. Potentials of mean force (PMFs) were obtained from umbrella-sampling data using Alan Grossfield's Weighted Histogram Analysis Method (WHAM) implementation, version 2.0.9 [34].

3. Results and discussion

3.1. Coiled coil dimers

The coiled coil is a biologically important structural pattern of helix–helix oligomerization in proteins [12]. The heptad repeat motif is a frequent driver of coiled coils; in it, residues in two or more α-helices interlock in a repeating hpphppp pattern, with hydrophobic residues (h) typically in the first and fourth positions and polar residues (p) in-between (charged residues are often found at the fifth and seventh positions) [12]. The heptad repeat is not a mere polarity matching motif: it leverages the spatial fitting of each helix's side-chains into inter-residue gaps in the other helices, in what Crick termed a 'knobs' into 'holes' pattern [35]. This structural matching further requires helices to become supercoiled, at 3.5 residues per turn, by slightly bending their axes in a left-handed fashion [12].

In our base systems, using either Martini 2 or Martini 3 versions, none of the expected coiled coil dimers formed correctly when compared to the experimentally obtained structures (Fig. 1). With Martini 2, dimers did form stably, but mostly incorrectly: the 1ZIK dimer formed in an antiparallel orientation, contrary to the parallel X-ray structure; the 1U0I dimer formed roughly as frequently in either orientation, with some of the replicate trajectories exhibiting a transition between the two states, but even when correctly parallel the peptides dimerized along a shifted and rotated interface (see the mismatch between the experimental and simulated contacts in Figs. 1A and 1B). Martini 2 dimers may have also been overstabilized in that after contact, no dissociation was observed in any of the replicates.

In contrast with Martini 2, Martini 3 displayed an interaction propensity between the peptides so low that no discernible predominant dimer structures were observed (Fig. 1A). This did not change when the peptides' structure was further restrained by an elastic network (see Supplementary Figure S1) — the elastic network alternative was tested in that it might better maintain the helices supercoiled, though for peptides this short the structural difference is still small. Even when Martini 3 peptides did transiently come into contact, they did so mostly via regions other than the correct dimerization interface.

We simulated additional systems in which peptides were started already in their dimerization pose (see Supplementary Figure S2). In these conditions, Martini 2 was able to retain the correct 1ZIK dimerization structure, whereas the 1U0I dimer tended to shift to an antiparallel configuration. This partial success with the 1ZIK dimer, and the difference to the observed results in Fig. 1, reflects the known excessive protein–protein interaction with Martini 2 [2]: the dimer is likely to become kinetically trapped close to whichever configuration it comes into contact as. This effect stabilizes correct and wrong interfaces alike, preventing an efficient inference of preferred poses from unbiased simulations.

Martini 3 systems were also simulated starting from bound configurations. A final tested condition, also starting from a bound state, combined the addition of elastic networks with side-chain orientation restraints to better match structural data [19]. In all of these cases

Martini 3 peptides behaved as in Fig. 1, with no significant dimerization (see Supplementary Figure S2).

Weaker peptide–peptide affinities were expected for Martini3, since one of its development goals was to mitigate the over-aggregation seen in Martini 2. However, to observe almost no dimeric contacts between peptides over an aggregate 80+ μs per system indicates that this type of short proteins now interacts too little. Even transient peptide contacts shunned most of the more hydrophobic correct dimer interface, to instead cluster around polar/charged residues (Fig. 1B). This hints at a possible overly hydrophilic character of the peptides. One of Martini 3's development decisions possibly related to this was the choice to model all backbone beads with the same polarity type (P2), regardless of secondary structure. In Martini 2 the backbone bead types in helical or sheet secondary structures (particle types, N0 and Nda, respectively) were the least polar among backbone types, much less than the random coil one (P5), and reflected a lower availability of the carbonyl and amide in establishing further hydrogen bonding [5]. Our observations are also in line with those of Lamprakis et al. [36] using the 'open-beta' development version of Martini 3 [37]. In that work, Martini 3 underestimated some aqueous protein association energies, and experimental interfaces were often not recovered.

In spite of our and others' observations, Martini 3 has been shown to successfully model helix association and the salting-in/salting-out effect of proteins in solution [3]. However, in those validation systems helix association was probed only for TM peptides/proteins; the protein–protein interaction imbalances at play in our tests may be mitigated in a membrane environment, as they already sometimes were in Martini 2 [2,8,36,38]. The salting-in/salting-out Martini 3 tests, however, were performed in solution, and yielded realistic degrees of aggregation for the villin headpiece (VH) and the mutated cellulose-binding domain from *Cellulomonas fimi* (CBD) [3,39,40]. Those proteins are only a few kDa larger than the coiled coil dimers in this work but are large enough to have well-defined tertiary structure and globular shape. This makes for larger interaction patches when oligomerizing compared to the almost linear interface between two single α-helices, and may compensate the factors that prevent Martini 3 from properly forming the short coiled coils. Additionally, neither VH nor CBD are fully α-helical/β-sheet structures (helices/sheets account for 70% and 57% of VH and CBD, respectively). If indeed backbone beads are overly polar in Martini 3 α-helices and β-sheets, the relative inaccuracy in overall protein hydrophilicity would then be greater in the 100% helical coiled coil peptides than in VH or CBD. If correct, our explanatory hypotheses for the lack of oligomerization would point to short, fully helical peptides as extreme cases for which Martini 3 selectivity breaks down.

3.2. Transmembrane WALP behavior

TM helices are an important structural aspect of protein–membrane interactions [41]. They are stabilized by such factors as hydrophobic matching (the length matching of helix and membrane hydrophobic spans), or the degree of charge/polarity of the helix's termini. The fluid nature of interactions between proteins and membranes further means that either component can adapt to non-optimal characteristics [42]: among other changes, excessively long helices – particularly if monomeric or at low degrees of oligomerization – will frequently tilt to better accommodate their hydrophobic span within the membrane core; at the same time, lipids vicinal to the protein may display a thicker bilayer profile, with a concomitant locally thicker core. Conversely, very short helices can induce a local thinning of membranes.

Using Martini 2 and 3 we simulated four α-helices 16, 19, 23, and 27 residues in length, from the WALP (tryptophan–alanine–leucine) series of peptides (termed WALP16, WALP19, WALP23, and WALP27; see Table 1). We chose these peptides because their TM behavior is well established, and their tilt angle as a function of their length has been documented experimentally and with atomistic simulations [13]. This was relevant because we wanted to probe the TM stability of
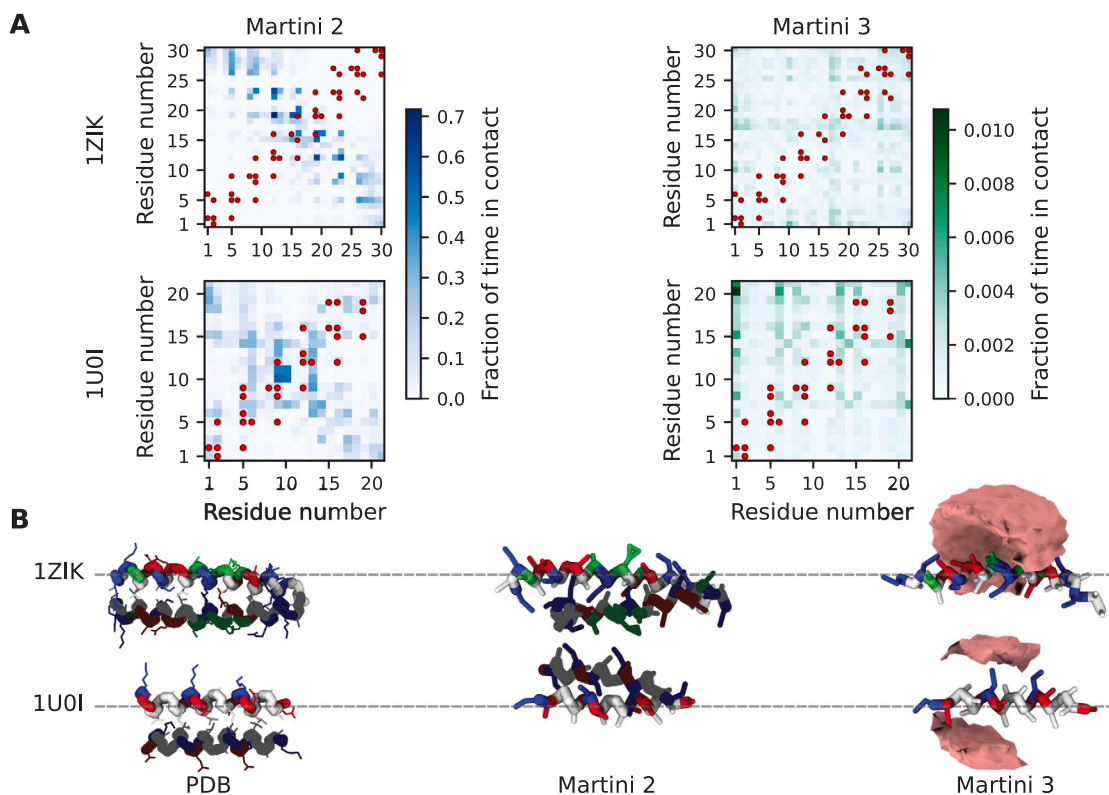
Fig. 1. Behavior of coiled coil peptides simulated using the Martini 2 and 3 models. Martini 3 results are shown for topologies without elastic networks (see Supplementary Figure S1 for the very similar behavior with elastic networks). A: Heat maps of contacts between the two monomers (for the 1U0I heterodimer, monomers A and B are in the *x* and *y* axes, respectively). Intensity represents the fraction of simulation time across replicates in which residues were within a 6 Å cutoff. Red dots represent experimentally-determined residue contacts (for the 1ZIK X-ray structure, residues within 5 Å; for the 1U0I NMR structure, residues within 4 Å in more than 6 of the 20 deposited minimum-energy models). B: Rendered images of the PDB structures and of representative Martini 2 dimers, with the same reference peptide aligned along a common axis (dashed line) for direct comparison (the parallel Martini 2 dimer was chosen in the 1U0I case); the second peptide is shown darkened, for better distinction. Martini 3 simulations did not indicate any preferred binding mode, and occupancies of the second peptide are represented instead (in pink, for values > 0.10%). Residues are color-coded white for apolar, green for uncharged polar, red for anionic and blue for cationic.

peptides, prompted by recent observations that supposedly transmembranar peptides might, under Martini 3, have weaker affinity for the transmembrane state [16,17]. Peptides were simulated embedded in a DMPC membrane, as in the atomistic simulations of Ref. [13], above the lipid's gel-to-fluid transition temperature.

In general, both Martini 2 and Martini 3 were able to recover the length–tilt dependence of WALPs — most visibly for WALP27, which is the longest of the tested peptides (Fig. 2). Martini 3 seems to be more sensitive in that WALP23 is also seen to tilt. This is in agreement with reported WALP23 behavior in DMPC [13] and is also an improvement over Martini 2, with which WALP23 does not significantly tilt. The DMPC membrane was also observed to become thinner near the peptides. With Martini 3, this occurred for all peptides, even the longer WALP27, whereas with Martini 2 WALP27 caused a small local thickening instead (see Supplementary Figure S3).

3.2.1. Transmembrane instability

In Martini 3 simulations, WALP16 was observed to consistently be ejected from the membrane core in the μs timescale (Fig. 2C and E). Of the three replicates, two were ejected towards the C-terminal leaflet and one towards the N-terminal leaflet. Such a movement did not occur with Martini 2, and is a behavior that is not supported by experimental results nor by simulations at higher resolutions.

We can preclude a possibly inaccurate thickness of the membrane as the cause for the WALP16 TM instability: due to its coarseness, the Martini 3 DMPC is the same model as the one representing DLPC, and yields a thickness between 2 and 3 Å thinner than experimentally reported [43] (3.4 nm vs 3.67 nm; see Supplementary Figure S3). Being somewhat thinner, a Martini DMPC membrane is, if anything, more

accommodating of WALP16's negative size mismatch than if it better matched the experimental thickness (moreover, the mismatch is further reduced by the additional thinning of lipids in the peptide's vicinity).

Another potential cause for WALP16's TM-to-adsorbed ejection could be the way we modeled the peptides' termini. Since neither Martini model has parameters for the WALPs' N-terminal acetylations or C-terminal *n*-methyl amidations, we simply considered each terminal bead to be uncharged, and did not add any extra particles. As a consequence, WALPs are marginally shorter than if termini caps had been explicitly modeled, which could have exacerbated the negative size mismatch of WALP16 beyond the point of TM stability. However, we were able to observe the same instability behavior, at a larger timescale, for one of the WALP19 replicates[1] (see Fig. 2C). If the shortening of termini caps were indeed the destabilizing aspect for WALP16, then WALP19, with 3 extra residues, should have remained transmembranar.

Having ruled out limitations specific to the membrane or WALP models, we are left to conclude that the pattern of Martini 3 protein–membrane affinities is offset in a way that favors the adsorbed state vs the TM state, while possibly also lowering the transmembranar-to-adsorbed energy barrier (the point when one of the peptide's polar ends is dragged across the hydrophobic bilayer core). Note that the same

---

[1] Observation of WALP19 TM instability was serendipitous in that it was first observed, at a shorter timescale, under wrong (isotropic) pressure coupling conditions. This prompted us to monitor WALP19 stability – with correct pressure coupling – into the 10^2 μs scale, and indeed the same behavior was seen as for WALP16.
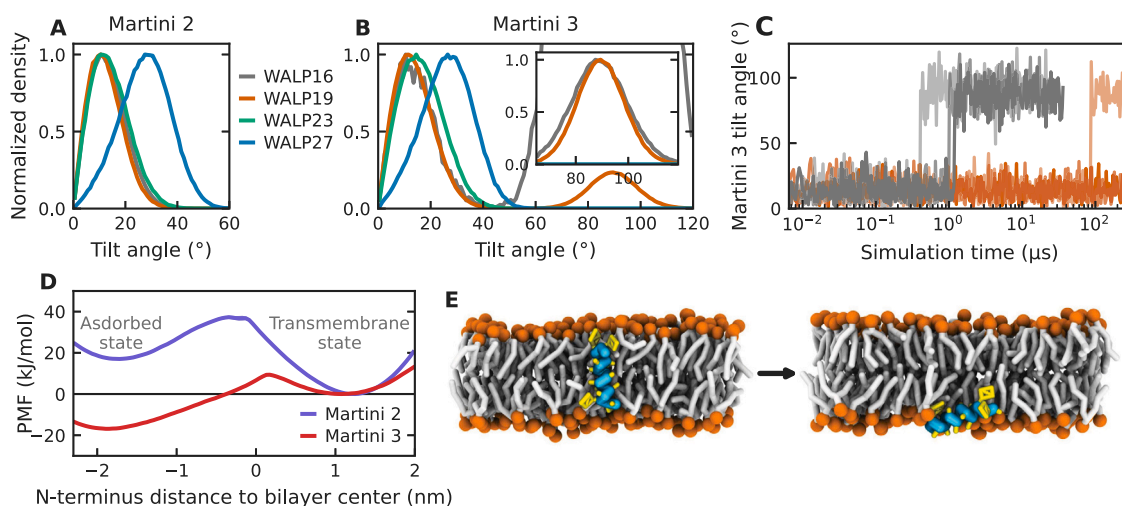
Fig. 2. Transmembrane behavior of WALPs in simulations with Martini 2 and 3. A and B: Martini 2 (A) and 3 (B) distributions of the WALP tilt angles (relative to the bilayer normal) within a DMPC membrane; data is shown aggregated from each peptide's three replicates, normalized to the distribution peak below 50°. With Martini 3, WALPs 16 and 19 leave the membrane core to become only adsorbed: the inset in B details this region of the tilt angle distribution, with data normalized to the peak above 50°. C: Kinetics of tilt angle variation over time for each replicate of Martini 3 simulations of WALP16 and WALP19 (replicates of a peptide are in different shades of the respective color from the legend of panels A/B). D: PMF of the TM-to-adsorbed transition of WALP16, expressed as a function of the distance of the N terminus to the bilayer center (confidence interval is indicated by shading, but it is never broader than ±0.6 kJ/mol); a TM state with N terminus in the top leaflet was used, as in panel E. Martini 3 not only has a lower energy barrier between states than Martini 2, its adsorbed state is also of overall lower energy than the TM state. E: Representative WALP16 configurations, simulated with Martini 3, before (left) and after (right) the peptide leaves the bilayer core for a membrane-adsorbed state (the peptide backbone is in blue, side-chains in yellow, and lipids in white tails with orange phosphate groups; solvent and part of the membrane were hidden, for clarity).

ejection behavior would not result from just the lowering of the energy barrier: were this the case, WALPs would as easily come back to the supposedly more favorable TM state, which is a transition we never observed (Fig. 2C).

Our interpretation is in line with recent Martini 3 simulations by Cabezudo and co-workers [17] of membrane self-assembly in the presence of a TM helix dimer. In those simulations, the dimer was effectively excluded from the membrane upon self-assembly. The dimer did remain transmembranar if inserted into pre-assembled membranes, though this may simply reflect a slow TM-to-adsorbed kinetic (in this regard, the simpler WALP systems are advantageous in that ejection events can be observed in the 10^0–10^2 μs scale).

Cabezudo and co-workers assign the erroneous behavior of Martini 3 to excessively strong peptide–water interactions [17], which parallels the excessive-hydrophilicity hypothesis we put forth above for the lack of aggregation of coiled coil dimers. Indeed, excessive protein–water interactions would selectively stabilize the water-exposed adsorbed state. They would also lower the TM-to-adsorbed energy barrier: as a peptide's end dives across the membrane core, it progressively allows residues on the opposite end to come into contact with increasing amounts of water; the water interactions of those residues, if too strong, then overly compensate the cost of moving the diving end's polar moieties through the core. Such a lowering of this energy barrier would then be the reason why we were able to observe TM peptide ejection in the μs scale.

From umbrella sampling simulations we obtained PMFs of the TM-to-adsorbed transition for Martini 2 and 3 (Fig. 2D; see sampling distributions in Supplementary Figure S4). The resulting energy landscapes neatly match the energetic aspects we hypothesized: Martini 3 has, compared to Martini 2, both a lower energy barrier to leave the TM state and a lower energy of the adsorbed state. Note that the Martini 3 adsorbed state is also more stable than its TM state by almost 20 kJ/mol; conversely, in Martini 2 the adsorbed state is more energetic by about 15 kJ/mol. These PMFs show that in Martini 3 the peptides are not becoming kinetically trapped in the adsorbed state, but rather that that is instead their preferred state.

3.3. Mitigation strategies

The correction of the Martini 3 protein–protein and protein–lipid interaction behavior we describe here requires a deeper characterization of the problem(s) at hand and, likely, some degree of re-parameterization of these types of molecules. In the meantime, some mitigating approaches can be employed to enable a more representative simulation of these kinds of systems.

3.3.1. Interaction scaling

By using a scaling factor to adjust cross interactions between molecules, or between them and water, one can centrally re-balance the affinities of an entire system. This strategy is not new, having been proposed to address the excessive protein aggregation under Martini 2 — either by decreasing protein–protein interactions [7,8] or by increasing protein–water ones [9].

Cabezudo and co-workers have proposed the scaling-down of protein–water interactions to stabilize Martini 3 TM peptide states [17]. The fact that they successfully employed this strategy reinforces that, indeed, a hydrophobicity/hydrophilicity imbalance is at play. The same strategy can, in principle, be applied to the coiled coil dimer systems: weakening protein–water interactions would certainly drive a stronger dimerization. It is unclear, however, whether a blanket scaling would be able to correct the apparent rejection of hydrophobic contacts seen in Fig. 1B.

Interaction scaling has the downside of impacting *all* adjusted interactions, and not only the ones responsible for the model's misbehavior. When defining scaled interactions, one also typically does not repeat the extensive testing that went into the force field's parameterization — the point being precisely to avoid such an in-depth redo. Because of these aspects, solutions involving interaction scaling have questionable transferability properties, and are better seen as temporary stopgap measures for the specific systems they were developed for.

3.3.2. System restraining

A second approach to driving simulations towards expected behavior is to use some sort of potential that restrains the phase space sampled by the simulations. In a general sense, this is already the case

of angle and dihedral bonded interactions in Martini, which account for the fact that the rest of CG interactions represent poorly intramolecular dynamics on their own.

A typical restraining strategy applied to Martini protein systems is the so-called elastic network [44], where several potentials restrain a set of distances between backbone particles to predefined values. Depending on their reach, elastic networks can restrain from secondary up to quaternary protein structures, and are therefore an adequate solution to simulating coiled coils as dimers.

With unstable TM peptides, restraints preventing the termini from diving into the bilayer core have also been successfully used [16]. This also requires restraining the membrane from buckling or from otherwise shifting significantly, else it may happen that the membrane becomes the one to leave the peptide.

The use of restraints has the advantage that the transferability properties of the model are generally not affected. This is particularly true if the system is restrained to a state that was already a local energy minimum and therefore only requires sporadic biasing (such as a TM peptide). The downsides of this approach relate to the loss of freedom in the restrained degrees of freedom: dynamic behavior involving the restrained dimensions becomes an input of the system, and no longer something that can be explicitly modeled or inferred. For instance, with elastic-networked coiled coils one would be unable to comment on monomer affinity or on their dynamics of pairing.

4. Conclusion

With our work we characterize important aspects of Martini 3 protein–protein and protein–membrane interactions and identify apparent shortcomings of the force field. By drawing attention to these points, and discussing several mitigation strategies, we aim to advise others studying related systems and hopefully limit the waste of researcher time and processor cycles on unproductive simulations.

Finally, given its young age, Martini 3 can be expected to still undergo several improvements. We hope our findings are a step towards such future developments.

CRediT authorship contribution statement

J. Karl Spinti: Data curation, Writing – original draft, Formal analysis, Visualization. **Fernando Neiva Nunes:** Data curation, Writing – original draft, Formal analysis, Visualization. **Manuel N. Melo:** Conceptualization, Supervision, Writing – original draft, Writing – review & editing, Methodology, Visualization.

Declaration of competing interest

The authors declare that they have no known competing financial interests or personal relationships that could have appeared to influence the work reported in this paper.

Data availability

Files used for simulating the systems, as well as contact and tilt-angle data in numerical form, are available for download from the Melo lab's website, at https://www.itqb.unl.pt/labs/multiscale-modeling.

Acknowledgments

Appendix A. Supplementary data

Supplementary material related to this article can be found online at https://doi.org/10.1016/j.cplett.2023.140436.

References

[1] S.J. Marrink, L. Monticelli, M.N. Melo, R. Alessandri, D.P. Tieleman, P.C.T. Souza, Two decades of Martini: Better beads, broader scope, WIREs Comput. Mol. Sci. (2022) e1620, http://dx.doi.org/10.1002/wcms.1620.

[2] R. Alessandri, P.C.T. Souza, S. Thallmair, M.N. Melo, A.H. de Vries, S.J. Marrink, Pitfalls of the Martini model, J. Chem. Theory Comput. 15 (10) (2019) 5448–5460, http://dx.doi.org/10.1021/acs.jctc.9b00473, pMID: 31498621.

[3] P.C.T. Souza, R. Alessandri, J. Barnoud, S. Thallmair, I. Faustino, F. Grünewald, I. Patmanidis, H. Abdizadeh, B.M.H. Bruininks, T.A. Wassenaar, P.C. Kroon, J. Melcr, V. Nieto, V. Corradi, H.M. Khan, J. Domański, M. Javanainen, H. Martinez-Seara, N. Reuter, R.B. Best, I. Vattulainen, L. Monticelli, X. Periole, D.P. Tieleman, A.H. de Vries, S.J. Marrink, Martini 3: A general purpose force field for coarse-grained molecular dynamics, Nature Methods 18 (2021) 382–388, http://dx.doi.org/10.1038/s41592-021-01098-3.

[4] S.J. Marrink, H.J. Risselada, S. Yefimov, D.P. Tieleman, A.H. de Vries, The martini force field: Coarse grained model for biomolecular simulations, J. Phys. Chem. B 111 (27) (2007) 7812–7824, http://dx.doi.org/10.1021/jp071097f, pMID: 17569554.

[5] L. Monticelli, S.K. Kandasamy, X. Periole, R.G. Larson, D.P. Tieleman, S.-J. Marrink, The Martini coarse-grained force field: Extension to proteins, J. Chem. Theory Comput. 4 (5) (2008) 819–834, http://dx.doi.org/10.1021/ct700324x, pMID: 26621095.

[6] D.H. de Jong, G. Singh, W.F.D. Bennett, C. Arnarez, T.A. Wassenaar, L.V. Schäfer, X. Periole, D.P. Tieleman, S.J. Marrink, Improved parameters for the Martini coarse-grained protein force field, J. Chem. Theory Comput. 9 (1) (2013) 687–697, http://dx.doi.org/10.1021/ct300646g, pMID: 26589065.

[7] A.C. Stark, C.T. Andrews, A.H. Elcock, Toward optimized potential functions for protein–protein interactions in aqueous solutions: Osmotic second virial coefficient calculations using the MARTINI coarse-grained force field, J. Chem. Theory Comput. 9 (9) (2013) 4176–4185, http://dx.doi.org/10.1021/ct400008p.

[8] M. Javanainen, H. Martinez-Seara, I. Vattulainen, Excessive aggregation of membrane proteins in the Martini model, PLoS One 12 (11) (2017) e0187936, http://dx.doi.org/10.1371/journal.pone.0187936.

[9] A.H. Larsen, Y. Wang, S. Bottaro, S. Grudinin, L. Arleth, K. Lindorff-Larsen, Combining molecular dynamics simulations with small-angle X-ray and neutron scattering data to study multi-domain proteins in solution, PLOS Comput. Biol. 16 (4) (2020) e1007870, http://dx.doi.org/10.1371/journal.pcbi.1007870.

[10] D. Lindhout, J. Litowski, P. Mercier, R. Hodges, B. Sykes, Nmr solution structure of a highly stable de novo heterodimeric coiled-coil, Biopolymers 75 (2004) 367–375, http://dx.doi.org/10.1002/bip.20150, pMID: 15457434.

[11] L. Gonzalez Jr., D. Woolfson, Buried polar residues and structural specificity in the gcn4 leucine zipper, Nat. Struct. Biol. 3 (1996) 1011–1018, http://dx.doi.org/10.1038/nsb1296-1011, pMID: 8946854.

[12] A.N. Lupas, J. Bassler, S. Dunin-Horkawicz, The structure and topology of α-helical coiled coils, in: Subcellular Biochemistry, Springer International Publishing, 2017, pp. 95–129, http://dx.doi.org/10.1007/978-3-319-49674-0_4.

[13] T. Kim, W. Im, Revisiting hydrophobic mismatch with free energy simulation studies of transmembrane helix tilt and rotation, Biophys. J. 99 (1) (2010) 175–183, http://dx.doi.org/10.1016/j.bpj.2010.04.015, pMID: 20655845.

[14] A. Holt, R. Koehorst, T. Rutters-Meijneke, M. Gelb, D. Rijkers, M. Hemminga, J. Killian, Tilt and rotation angles of a transmembrane model peptide as studied by fluorescence spectroscopy, Biophys. J. 97 (8) (2009) 2258–2266, http://dx.doi.org/10.1016/j.bpj.2009.07.042, pMID: 19843458.

[15] M. de Planque, J. Killian, Tilt and rotation angles of a transmembrane model peptide as studied by fluorescence spectroscopy, Mol. Membr. Biol. 20 (4) (2003) 271–284, http://dx.doi.org/10.1080/09687680310001605352, pMID: 14578043.

[16] M. Valério, D.A. Mendonça, J. Morais, C.C. Buga, C.H. Cruz, M.A. Castanho, M.N. Melo, C.M. Soares, A.S. Veiga, D. Lousa, Parainfluenza fusion peptide promotes membrane fusion by assembling into oligomeric porelike structures, ACS Chem. Biol. (2022) null, http://dx.doi.org/10.1021/acschembio.2c00208, pMID: 35500279.

[17] A.C. Cabezudo, C. Athanasiou, A. Tsengenes, R.C. Wade, Scaling protein-water interactions in the Martini 3 coarse-grained force field to simulate transmembrane helix dimers in different lipid environments, 2022, http://dx.doi.org/10.1101/2022.09.09.506752, bioRxiv.

[18] P. Kroon, Aggregate, Automate, Assemble, University of Groningen, ISBN: 978-94-034-2581-8, 2020, pp. 16–53, Ch. Martinize 2 -VerMoUTH.

[19] F.A. Herzog, L. Braun, I. Schoen, V. Vogel, Improved side chain dynamics in Martini simulations of protein–lipid interfaces, J. Chem. Theory Comput. 12 (5) (2016) 2446–2458, http://dx.doi.org/10.1021/acs.jctc.6b00122.

[20] M.D. Hanwell, D.E. Curtis, D.C. Lonie, T. Vandermeersch, E. Zurek, G.R. Hutchison, Avogadro: An advanced semantic chemical editor, visualization, and analysis platform, J. Cheminform. 4 (17) (2012).

[21] T.A. Wassenaar, H.I. Ingólfsson, R.A. Böckmann, D.P. Tieleman, S.J. Marrink, Computational lipidomics with insane: A versatile tool for generating custom membranes for molecular simulations, J. Chem. Theory Comput. 11 (5) (2015) 2144–2155, http://dx.doi.org/10.1021/acs.jctc.5b00209, pMID: 26574417.

[22] M.J. Abraham, T. Murtola, R. Schulz, S. Páll, J.C. Smith, B. Hess, E. Lindahl, Gromacs: High performance molecular simulations through multi-level parallelism from laptops to supercomputers, SoftwareX 1-2 (2015) 19–25, http://dx.doi.org/10.1016/j.softx.2015.06.001.

[23] D.H. de Jong, S. Baoukina, H.I. Ingolfsson, S.J. Marrink, Martini straight: Boosting performance using a shorter cutoff and GPUs, Comput. Phys. Comm. 199 (2016) 1–7, http://dx.doi.org/10.1016/j.cpc.2015.09.014.

[24] G. Bussi, D. Donadio, M. Parrinello, Canonical sampling through velocity rescaling, J. Chem. Phys. 126 (1) (2007) 014101, http://dx.doi.org/10.1063/1.2408420.

[25] M. Parrinello, R. A., Polymorphic transitions in single crystals: A new molecular dynamics method, J. Appl. Phys. 52 (12) (1981) 7182–7190, http://dx.doi.org/10.1063/1.328693.

[26] H.J.C. Berendsen, J.P.M. Postma, W.F. van Gunsteren, A. DiNola, J.R. Haak, Molecular dynamics with coupling to an external bath, J. Chem. Phys. 81 (8) (1984) 3684–3690, http://dx.doi.org/10.1063/1.448118.

[27] N. Michaud-Agrawal, E.J. Denning, T.B. Woolf, O. Beckstein, Mdanalysis: A toolkit for the analysis of molecular dynamics simulations, J. Comput. Chem. 32 (10) (2011) 2319–2327, http://dx.doi.org/10.1002/jcc.21787.

[28] R.J. Gowers, Max Linke, Jonathan Barnoud, Tyler J.E. Reddy, Manuel N. Melo, Sean L. Seyler, Jan Domański, David L. Dotson, Sébastien Buchoux, Ian M. Kenney, O. Beckstein, Mdanalysis: A Python package for the rapid analysis of molecular dynamics simulations, in: S. Benthall, S. Rostrup (Eds.), Proceedings of the 15th Python in Science Conference, 2016, pp. 98–105, http://dx.doi.org/10.25080/Majora-629e541a-00e.

[29] C.R. Harris, K.J. Millman, S.J. van der Walt, R. Gommers, P. Virtanen, D. Cournapeau, E. Wieser, J. Taylor, S. Berg, N.J. Smith, R. Kern, M. Picus, S. Hoyer, M.H. van Kerkwijk, M. Brett, A. Haldane, J.F. del Río, M. Wiebe, P. Peterson, P. Gérard-Marchant, K. Sheppard, T. Reddy, W. Weckesser, H. Abbasi, C. Gohlke, T.E. Oliphant, Array programming with NumPy, Nature 585 (7825) (2020) 357–362, http://dx.doi.org/10.1038/s41586-020-2649-2.

[30] J.D. Hunter, Matplotlib: A 2d graphics environment, Comput. Sci. Eng. 9 (3) (2007) 90–95, http://dx.doi.org/10.1109/MCSE.2007.55.

[31] W. Humphrey, A. Dalke, K. Schulten, VMD – Visual molecular dynamics, J. Mol. Graph. 14 (1996) 33–38.

[32] M. Bansal, S. Kumart, R. Velavan, HELANAL: A program to characterize helix geometry in proteins, J. Biomol. Struct. Dyn. 17 (5) (2000) 811–819, http://dx.doi.org/10.1080/07391102.2000.10506570.

[33] P. Smith, C.D. Lorenz, Lipyphilic: A python toolkit for the analysis of lipid membrane simulations, J. Chem. Theory Comput. 17 (9) (2021) 5907–5919, http://dx.doi.org/10.1021/acs.jctc.1c00447.

[34] A. Grossfield, WHAM: The weighted histogram analysis method, version 2.0.9, 2017, URL http://membrane.urmc.rochester.edu/wordpress/?page_id=126.

[35] F.H.C. Crick, Is α-keratin a coiled coil? Nature 170 (4334) (1952) 882–883, http://dx.doi.org/10.1038/170882b0.

[36] C. Lamprakis, I. Andreadelis, J. Manchester, C. Velez-Vega, J.S. Duca, Z. Cournia, Evaluating the efficiency of the Martini force field to study protein dimerization in aqueous and membrane environments, J. Chem. Theory Comput. 17 (5) (2021) 3088–3102, http://dx.doi.org/10.1021/acs.jctc.0c00507.

[37] Martini 3 open-beta, 2018, URL http://www.cgmartini.nl/index.php/martini3beta.

[38] J. Su, S.J. Marrink, M.N. Melo, Localization preference of antimicrobial peptides on liquid-disordered membrane domains, Front. Cell Dev. Biol. 8 (2020) http://dx.doi.org/10.3389/fcell.2020.00350.

[39] J. Meng, D. Vardar, Y. Wang, H.-C. Guo, J.F. Head, C.J. McKnight, High-resolution crystal structures of villin headpiece and mutants with reduced f-actin binding activity, Biochemistry 44 (36) (2005) 11963–11973, http://dx.doi.org/10.1021/bi050850x.

[40] C. Højgaard, C. Kofoed, R. Espersen, K.E. Johansson, M. Villa, M. Willemoës, K. Lindorff-Larsen, K. Teilum, J.R. Winther, A soluble, folded protein without charged amino acid residues, Biochemistry 55 (28) (2016) 3949–3956, http://dx.doi.org/10.1021/acs.biochem.6b00269.

[41] R.W. Albers, Chapter 2 - cell membrane structures and functions, in: S.T. Brady, G.J. Siegel, R.W. Albers, D.L. Price (Eds.), Basic Neurochemistry (Eighth Edition), eighth ed., Academic Press, New York, 2012, pp. 26–39, http://dx.doi.org/10.1016/B978-0-12-374947-5.00002-X.

[42] J. Killian, Hydrophobic mismatch between proteins and lipids in membranes, Biochim. Biophys. Acta (BBA) - Rev. Biomembranes 1376 (3) (1998) 401–416, http://dx.doi.org/10.1016/s0304-4157(98)00017-3.

[43] N. Kučerka, M.-P. Nieh, J. Katsaras, Fluid phase lipid areas and bilayer thicknesses of commonly used phosphatidylcholines as a function of temperature, Biochim. Biophys. Acta (BBA) - Biomembr. 1808 (11) (2011) 2761–2771, http://dx.doi.org/10.1016/j.bbamem.2011.07.022.

[44] X. Periole, M. Cavalli, S.-J. Marrink, M.A. Ceruso, Combining an elastic network with a coarse-grained molecular force field: Structure, dynamics, and intermolecular recognition, J. Chem. Theory Comput. 5 (9) (2009) 2531–2543, http://dx.doi.org/10.1021/ct9002114.